International Journal of Innovative Computing, Information and Control
Volume **15**, Number **1**, February **2019**

 ISSN 1349-4198
pp. 1–20

HYBRID ADAPTIVE NOTCH FILTER AND FIXED-STRUCTURE PID H_∞ ROBUST LOOP SHAPING CONTROL BASED PSO FOR HARD DISK DRIVE SERVO ACTUATOR

Poom Konghuayrob[1], Somyot Kaitwanidvilai[1] and Hisayuki Aoyama[2]

[1]Department of Electrical Engineering
Faculty of Engineering
King Mongkut's Institute of Technology Ladkrabang
Chalongkrung Rd., Ladkrabang, Bangkok 10520, Thailand
{ poom.konghuayrob; drsomyotk }@gmail.com

[2]Department of Mechanical Engineering and Intelligent Systems
The University of Electro-Communications
1-5-1 Chofugaoka, Chofu, Tokyo 182-8585, Japan
aoyama@net.aolab.mce.uec.ac.jp

Received April 2018; revised August 2018

Abstract. *In order to achieve the high precision head-positioning of the voice coil motor (VCM) actuator with narrow track pitch, the adaptive notch filter based limited-search-range of particle swarm optimization (PSO), as well as the fixed-structure propor-tional-integral-derivative H_∞ robust loop shaping controller using the concept of four closed loop disturbance norms is proposed. Generally the conventional method, fixed-frequency notch filter (FFNF), is combined with the nominal plant to reduce the effect of the mechanical vibration resonance; however, the resonance mode of servo system can be shifted with various factors such as the ambient temperature change, and the unbalanced disk. In addition, mathematical solving in the H_∞ robust control problems and the suitable notch filter design are very complex and the final results of the conventional controller with notch filters are normally complicated structure and high order which is difficult to implement. Thus, the adding of intelligent system in the proposed design with the careful range of the search space is utilized to suppress the vibration caused by resonance mode shifting and also reduce the order of the final robust controller. Simulation results of six scenarios test demonstrate the effectiveness of the proposed design compared with FFNF in the commercial product.*

Keywords: Adaptive notch filter, Fixed-structure H_∞ robust control, PSO, Hard disk drive, Resonance shifted

1. **Introduction.** Since the most significant trend of data storage capacity in hard disk drive (HDD) has grown around 30%-40% per year, increasing in areal density is also required. The near future target of the HDD capacity is to break 10 Tbit/in^2, which means that the decreasing of track pitch to around 11.6 nm desires a track mis-registration (TMR) budget less than 1.39 nm (3-sigma value) [1]. The major TMR sources consist of spindle runout, disk fluttering, bias forces, the actuator pivot friction, PES noise, the written-in repeatable runout and residual actuator, suspension vibration due to seek/setting, the external vibration/shock disturbances including arm and suspension vibrations due to the air turbulence [2,3]. This trend leads to an improvement of the read/write head positioning system. Because of the narrow track pitch and disturbances, it is difficult to control the actuator to achieve both fast and accurate head positioning over

DOI: 10.24507/ijicic.15.01.1

the target tracks. Therefore, the high precision and high performance control methods such as robust control, adaptive controller design, including the attenuation of vibration resonance compensation are considered to eradicate the effect of external disturbances and measurement noises. Most suggestions of the controller design in several researches were proposed in [1-6,9-17], and the servo system controller was needed to be designed for high bandwidth. Unfortunately, the servo bandwidth is limited by the mechanical resonance mode of the actuator, which causes large oscillations to the closed loop system response.

VCM is used to move the head positioning to the desired target track in the track seeking process, and it generates torque applied to the primary stage of the servo mechanism [3]. To generate this torque, the proportional current is injected to the coil of the VCM in hard disk drive, which causes the pivoted actuator arm to move. This paper focuses on the development of control system for the VCM.

Since over the past two decades, H_∞ control is the popular technique in the fields of robust control. It is the modern control technique which has high potential to design robust controllers for achieving stability and guaranteeing performance of the system. In addition, there are some successful experiments of the H_∞ control [9-15]; however, these controllers were designed with the complex structures and high-order. The orders of nominal plant and weighting compensation are the main factors of the controller order. Additionally, the solving of mathematic equations which are two Riccati's equations in this optimal control problem along with the controller structure constraint is not easy. Thus, the specified structure of controller has been proposed to overcome the problem of high controller order [9,14]; in their techniques, they applied the intelligent systems such as genetic algorithm (GA), particle swarm optimization (PSO) to solving the non-convex problem in their controller designs and applied to the various systems such as Himat air craft, pneumatic robot arm, and power system. The HDD application in [14] proposed the robust controller design with the fixed-frequency notch filter (FFNF) which is effective for VCM actuator; however, in case of the perturbation plant caused by the shifted frequencies which exists far away from the nominal plant, the controller as proposed in [14] is not good enough to maintain the stability of HDD system. In addition, to solve mathematical problem for achieving the high robust performance in real time is not applicable due to the long computational time in the design process.

The adaptive control is one of the effective methods to maintain the system stability under the uncertainties constraint, which were proposed in [16-19]. In [19], the selected notch filters of their adaptation process were updated until the frequency response characteristics with notch filters were suitable; additionally, authors in [18] proposed a tunable finite-duration impulse response (FIR) filter in their design in order to identify the resonance frequencies position of each actuator. Their method adapted the center frequency of interested resonant mode by using a self-regulating manner. The application of a discrete time adaptive resonance compensator with the adjusted uncertain resonance in HDD actuator was presented in [19]. The proposed technique applied the discrete linearity of the parallel modeling structure with known and unknown nominal resonance mode to calculating the VCM output error between actual and desired output, and then applied this error to evaluating the adaptive signal in order to prevent the nominal control from the plant cancelation effect. However, these adaptive techniques still require the high time-consuming to calculate the results such as Fourier transform and the complex mathematic solving in the adaptation term of the adaptive process. Furthermore, the implemented controller in the HDD system needs a fast calculation along with the high speed settling time requirement. In order to overcome these problems, the simple solution solving of

the complicated mathematical calculation is considered in the proposed technique. The proposed method is different from the above-mentioned ones with the motivations as:

1) To design the robust controller with fixed-structure PID based on H_∞ robust loop shaping method for attenuating the effect of disturbance including the measurement noise properly, additionally, the controller with the PID structure is easily implemented for performance improvement of the considered HDD servo system.

2) To apply the simplified adaptive notch filter with the proposed design fixed-structure robust PID in order to increase the system stability and reduce the oscillation caused by resonance frequencies shift. The proposed adaptive notch filter is updated online by using the particle swarm optimization algorithm in adaptation process to search the suitable center of the resonance frequency in order to suppress the unwanted resonance frequency gain.

This paper is organized as follows. Section 2 details the dynamic model of the VCM with resonance modes, the resonance suppression and the notch filter compensation. Section 3 describes the H_∞ robust loop shaping design and the proposed fixed-structure loop shaping based PSO synthesis including the controller synthesized steps of each controller. Section 4 presents the concept of the proposed adaptive notch filter, in which the nonlinear problems and complicated solution are solved by PSO. In Section 5, the simulation results of the proposed controllers and adaptive notch filter are illustrated. The summary and conclusion of the results including the future work are given in Section 6.

2. **Voice Coil Motor (VCM) Modeling and Notch Compensator.** The hard disk drive servo system as shown in Figure 1 is an electromagnetic device comprising a voice coil motor (VCM), the current driver amplifier and resonance model. The diverse high frequency resonance modes which affect the stability of the system can be explained by the characteristic of the VCM dynamic model. Moreover, in the pivot-bearing operation, unbalance spindle motor including windage is the cause of the nonlinear characteristic of hard disk servo system. These parameters need to be considered for modeling the VCM plant.

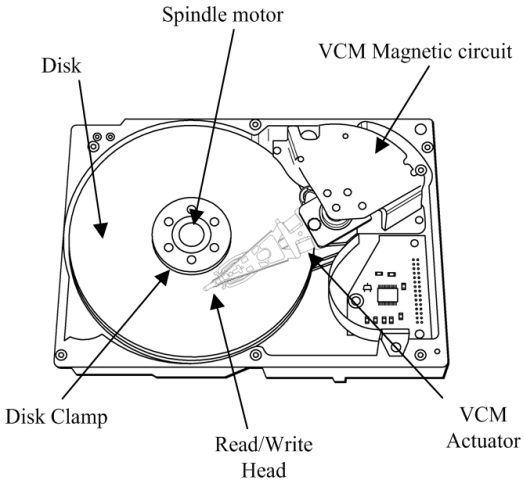

FIGURE 1. HDD with VCM actuator

The principle transfer function of VCM plant and its power driver without the resonance modes after taking the Laplace transform of its circuit analysis can be written as:

$$\frac{\theta(j\omega)}{u(j\omega)} = \frac{\frac{R_m k_a}{k_b}}{s(s\tau_e + 1) + (s\tau_a + 1)\left[s\tau_m + \frac{R_m}{(R_m + R_s)}\right]} \tag{1}$$

where θ is the position of the actuator in radian, u is the voltage input, R_m, R_s, k_a, k_b, τ_a, τ_e and τ_m are the VCM resistance, the parallel resistance, steady state gain, back emf force coefficient, amplifier, electrical and mechanical time constant, respectively. The details described in [20] show that the τ_a and τ_e are much smaller than τ_m and $R_s >> R_m$, additionally, θ which is the position of VCM can be transformed to tracks as:

$$G(j\omega) = \frac{y(j\omega)}{u(j\omega)} = \left(\frac{k_t k_a}{J}\right)\left(L_{VCM}\frac{TPI}{254e4}\right)\frac{1}{(j\omega)^2} = k_v k_y \frac{1}{(j\omega)^2} \tag{2}$$

where k_v is the acceleration constant, k_y is the position measurement gain, L_{VCM} is the length of the VCM actuator arm and TPI represents the track per inch of the VCM model. In addition, the overall VCM model, which consists of the resonance and the principle modeling characterized above, can be combined to the realistic VCM model actuator as:

$$G_{VCM}(j\omega) = \frac{k_v k_y}{(j\omega)^2} G_{resonance}(j\omega) \tag{3}$$

where $G_{resonance}$ is the resonance mode transfer function, and its structure can be formulated as:

$$G_{resonance}(j\omega) = \prod_{i=1}^{N} \frac{a_i(j\omega)^2 + b_i(j\omega) + \omega_i^2}{(j\omega)^2 + 2\xi_i\omega_i(j\omega) + \omega_i^2} \tag{4}$$

where a_i, b_i, ξ_i and ω_i are the coefficients of the i^{th} resonance dynamic.

VCM model as proposed in this paper based on the commercial hard disk assembly (HDA) detailed in [4], the VCM actuator parameters with four resonance modes at 1200, 2200, 4000 and 9000 Hz are classified as shown in Table 2 of the appendix section. Notch is utilized for decreasing the high frequency resonance effect which can be modeled as Equation (5). Moreover, the VCM plant has the two major resonance peak gains in the open loop of HDA frequency response. Thus, only two frequencies notch filter is reasonable to compensate the disadvantages of the resonance peaks.

$$N_{r,i}(j\omega) = \prod_{i=1}^{N} \frac{(j\omega)^2 + 2\xi_{inn}\omega_{ni}(j\omega) + \omega_{ni}^2}{(j\omega)^2 + 2\xi_{idn}\omega_{ni}(j\omega) + \omega_{ni}^2} \tag{5}$$

where ξ_{inn}, ξ_{idn} and ω_{ni} are coefficients of the i^{th} notch dynamic model.

Figure 2 illustrates the feedback control structure of VCM actuator with FFNF. As seen in the figure, the proposed controller is added to increase the tracking performance of the system, while the notch filter is used to degrade the major resonance effect of the plant model. In order to model the VCM and notch filter plant, the parameters of the 9^{th} order with four resonance modes of dynamic HDD and the FFNF detailed in the notch part of Table 1 are substituted in Equations (4) and (5), and then the results are shown in Equations (6) and (7) for HDD and notch filter dynamic model, respectively.

$$G_{VCM}(s) = \left\{ \frac{\begin{array}{c} 1.544\times10^{09}s^7 + 1.051\times10^{15}s^6 + 3.087\times10^{18}s^5 + 2.202\times10^{24}s^4 \\ + 9.03\times10^{26}s^3 + 3.886\times10^{32}s^2 + 1.723\times10^{34}s + 7.466\times10^{37} \end{array}}{\begin{array}{c} s^9 + 3273s^8 + 4.023\times10^{09}s^7 + 9.74\times10^{12}s^6 + 2.754\times10^{18}s^5 + 2.04 \\ \times10^{21}s^4 + 3.866\times10^{26}s^3 + 2.217\times10^{28}s^2 + 7.488\times10^{31}s + 9.332\times10^{32} \end{array}} \right\} \tag{6}$$

The dynamic model of the fixed-frequency notch filter can be written as:

$$N_r(s) = \left\{ \frac{s^4 + 2617s^3 + 3.831\times10^9 s^2 + 6.825\times10^{12}s + 2.016\times10^{18}}{s^4 + 50284s^3 + 4.437\times10^9 s^2 + 8.344\times10^{13}s + 2.016\times10^{18}} \right\} \tag{7}$$

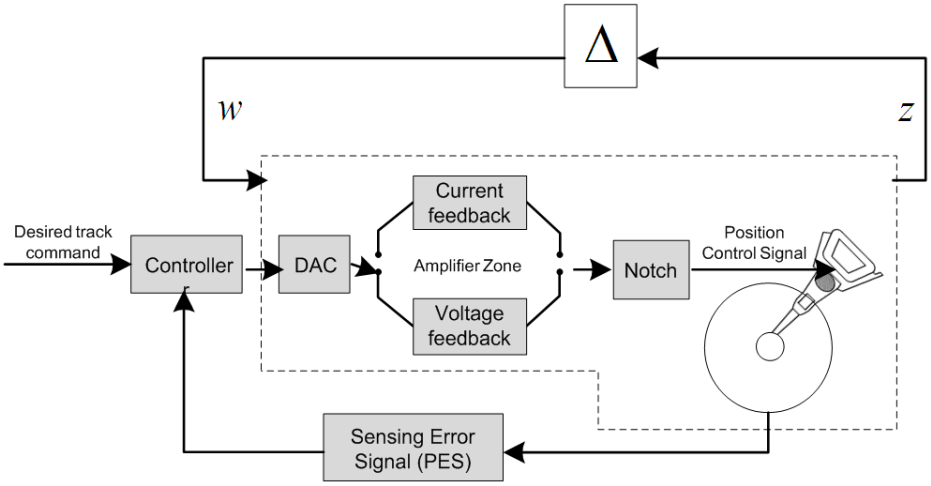

FIGURE 2. The feedback control structure of VCM actuator with fixed-frequency notch filter and plant uncertainty

TABLE 1. The performance and robustness specifications of the designed controller

Parameter	Value
k_t VCM, k_v VCM	20, 5.04e4
(a_1, b_1, ξ_1, ω_1 [Hz]) VCM	$(0.0000115, -0.00575, 0.05, 700)$
(a_2, b_2, ξ_2, ω_2 [Hz]) VCM	$(0, 0.023, 0.005, 2200)$
(a_3, b_3, ξ_3, ω_3 [Hz]) VCM	$(0, 0.8185, 0.05, 4000)$
(a_4, b_4, ξ_4, ω_4 [Hz]) VCM	$(0.0273, 0.1642, 0.005, 9000)$
(ξ_{1nn}, ξ_{1dn}, ω_{n1} [Hz]) NOTCH	$(0.0335, 1.674, 4000)$
(ξ_{2nn}, ξ_{2dn}, ω_{n2} [Hz]) NOTCH	$(0.2521, 2.521, 9000)$

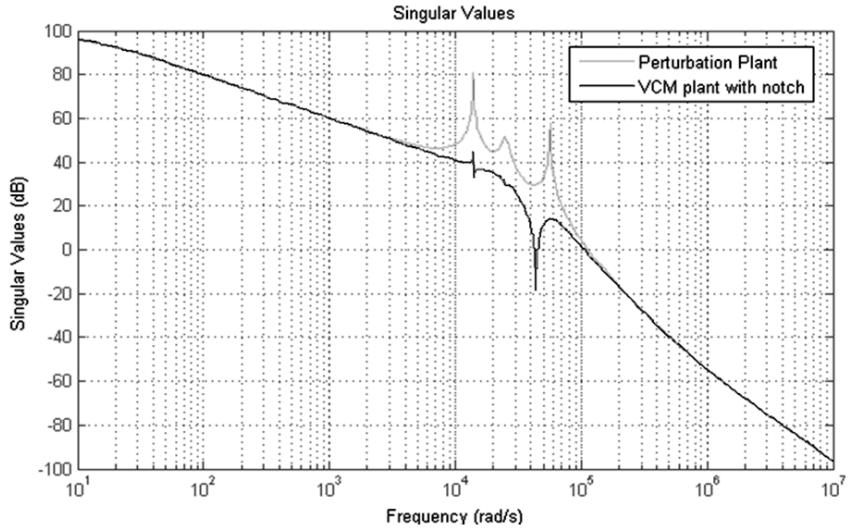

FIGURE 3. VCM actuator with fixed frequency notch filter (black line) and perturbed plant (light gray line)

Moreover, singular values of VCM with FFNF plant and the disturbed plant are illustrated in Figure 3. It is clear to show the advantage of notch filter for suppressing the unwanted resonance peak gain (black line) and the effect of disturbance from resonance shifted (light gray line).

3. H_∞ Loop Shaping and the Proposed Design.

3.1. Robust stabilization with normalized co-prime factors uncertainty [5,6].

Robust control is the method to stabilize the system, though it is perturbed by the disturbance and measurement noise and its internal parameters change. The robust control has been applied in many fields of control theory, including the loop shaping method. The shaped plant can be constituted as the transfer function, which contains the normalized nominator and denominator with robust left co-prime factorization ($G_s = M^{-1}N$). Furthermore, the system also consists of the various uncertainty models corresponding to the nominator (Δ_N) and denominator (Δ_M) of the considered system as characterized in Equation (8) as well. The system that comprises the uncertainties and the normalized co-prime factor characteristic can be described in Figure 4.

$$G_\Delta = (M + \Delta_M)^{-1}(N + \Delta_N) \tag{8}$$

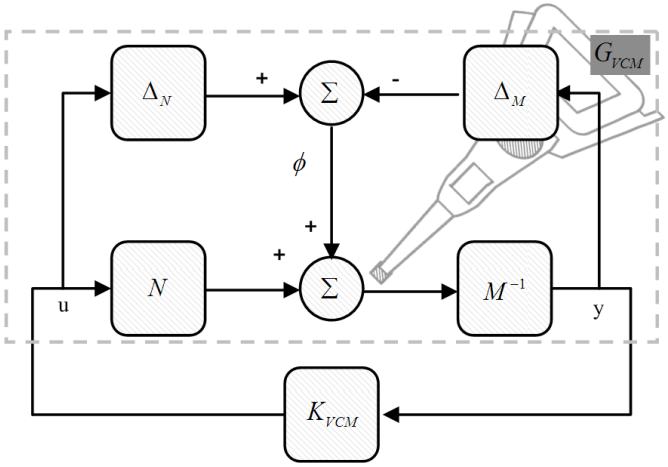

FIGURE 4. Closed loop control of left co-prime factorization uncertainty

To stabilize the system for covering the family of plant perturbation, the system uncertainty needs to be minimized as:

$$G_\Delta = \left\{(N_s + \Delta_{Ns})(M_s + \Delta_{Ms})^{-1} : \|\Delta_{Ns}\Delta_{Ms}\|_\infty < \varepsilon\right\} \tag{9}$$

where $\underset{s}{\tilde{N}}$, $\underset{s}{\tilde{M}}$, $\underset{Ns}{\tilde{\Delta}}$, $\underset{Ms}{\tilde{\Delta}} \in \Re H_\infty$ and ε is the uncertainty boundary called stability margin. The ε of the system should be maximized to guarantee the robustness of the system.

Based on the small gain theorem, the feedback system is robustly stable if (G, K) is internally stable and meets the requirement in Equation (10).

$$\left\| \begin{array}{c} K(I + GK)^{-1}M^{-1} \\ (I + GK)^{-1}M^{-1} \end{array} \right\|_\infty \leq \frac{1}{\varepsilon} \tag{10}$$

The robust controller K of the system G needs to minimize the $\gamma = \varepsilon^{-1}$, which is calculated from the following equation:

$$\gamma = \left\| \left[\begin{array}{c} K \\ I \end{array} \right] (I + GK)^{-1}M^{-1} \right\|_\infty \tag{11}$$

where γ is the infinity norm from ϕ to $[u, y]$ as appearing in Figure 5, and $(I + GK)^{-1}$ is the sensitivity function of the negative feedback system. The minimum achievable γ value corresponding to the stability margin is given as:

$$\gamma_{\min} = \varepsilon_{\max}^{-1} = 1 - \left\{\|[N\ M]\|_H^2\right\}^{0.5} = (1 + \lambda_{\max}(XZ))^{0.5} \tag{12}$$

where $\| \cdot \|_H$ represents the Hakel norm of the system, $\lambda_{\max}$ is the maximum eigenvalue of the matrix X multiplied by the matrix Z, while X and Z are the unique positive definite solutions to the algebraic Riccati Equations (13) and (14).

$$\begin{gathered}\left(A-BS^{-1}D^TC\right)Z+Z\left(A-BS^{-1}D^TC\right)^T-ZC^TR^{-1}CZ+BB^TS^{-1}=0\\ R=I+DD^T,\quad S=I+D^TD\end{gathered} \tag{13}$$

$$(A-BS^{-1}D^TC)^TX+X(A-BS^{-1}D^TC)-XB^TS^{-1}BX+C^TR^{-1}C=0 \tag{14}$$

where A, B, C and D represent the shaped plant in the state space form. The controller, which achieved that

$$\left\| \begin{array}{c} K(I+GK)^{-1}M^{-1} \\ (I+GK)^{-1}M^{-1} \end{array} \right\|_\infty \leq \gamma \tag{15}$$

for selected $\gamma < \gamma_{\min}$ can be synthesized by

$$K_\infty = \left[\begin{array}{cc} A+BF+\gamma^2(L^T)^{-1}ZC^T(C+DF) & \gamma^2(L^T)^{-1}ZC^T \\ B^TX & -D^T \end{array} \right] \tag{16}$$

where

$$F=-S^{-1}\left(D^TC+B^TX\right) \tag{17}$$

$$L=\left(1-\gamma^2\right)I+X \tag{18}$$

3.2. ***H_∞* loop shaping design procedure.** As seen in Figure 5, the nominal plant of hard disk drive is shaped with the proper weights and then the result of shaped plant is formulated with respect to co-prime factor uncertainty. The H_∞ design aims to achieve a balance of performance, robustness and stability of the closed loop system, properly.

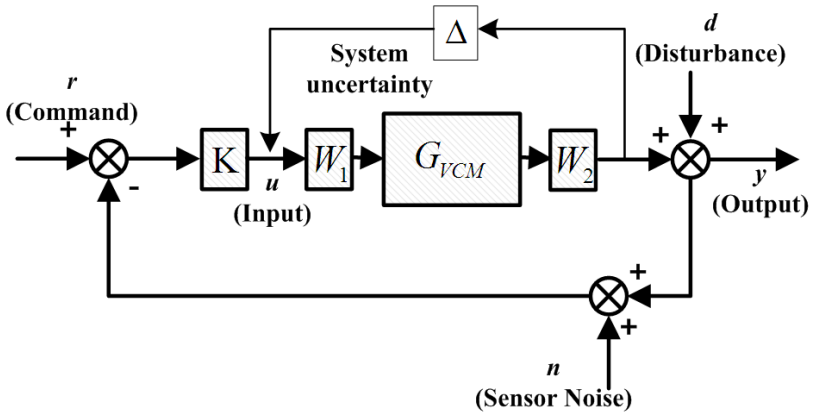

FIGURE 5. The loop shaping technique with HDD plant

Loop shaping is the procedure to design the robust controller based on H_∞ robust stabilization combined with the classical loop shaping attributed by McFarlane and Glover [7]. The concept of the H_∞ robust loop shaping is to augment the open loop plant by W_1 (pre-compensation) and/or W_2 (post-compensation) for achieving the desired singular values of open loop frequency response as seen in Figure 5. The shaped HDD plant can be formulated as:

$$G_S = W_1 G_{VCM} W_2 = M_s N_s^{-1} \tag{19}$$

The procedure to design H_∞ loop shaping can be summarized as follows [7].

- Specify the pre (W_1) and post (W_2) compensators to achieve the desired open loop singular frequency response. W_1 is utilized for getting a high gain at low-frequency to reject disturbance at both input and output of the plant, while W_2 is utilized for getting a low gain at high-frequency in order to reject the noise. Moreover, the shaped plant should get enough crossover frequency to achieve high bandwidth and fast settling time.
- Calculate the maximum stability margin $\varepsilon_{\max}$ with respect to co-prime factor uncertainties by using H_∞ optimization to solve the Riccati Equation (12). The suggestion of McFarlane and Glover in [7] described that if the calculated $\gamma_{\min} < 4$, it can be shown theoretically that the shaped plant of the open loop singular value is proper with this selected weighting function. If $\gamma_{\min} \geq 4$, return to step 1, and then redesign the new weights until achieving the requirement of the system.
- Synthesize the K_∞ controller by selecting the inverse stability margin γ slightly less than $\gamma_{\min}$, which the final controller structured can be illustrated in Figure 6 and written as:

$$K_{FINAL} = W_1 K_\infty W_2 \tag{20}$$

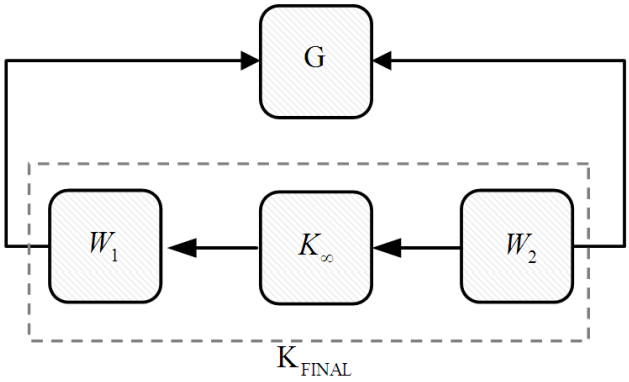

FIGURE 6. H_∞ robust loop shaping controller

3.3. **Fixed-structure H_∞ robust loop shaping controller design using PSO.** The famous PID controller is the most widely used control technique in various industrial applications, including the hard disk drive industry. The proposed 2nd order PID structure is designed by the H_∞ robust loop shaping procedure to synthesize the proposed fixed-structure robust controller for controlling the voice coil motor actuator of HDD. In addition, the proposed controller in this paper achieves the robustness according to the concept of a conventional H_∞ loop shaping and also gains the advantages in terms of reducing the computational time and high order of K_∞. In order to synthesize the controller with the proposed technique, the H_∞ controller (K_∞) in Equation (20) is inverted as:

$$K_\infty(s) = W_1^{-1}(s) K_{FINAL}(s) W_2^{-1}(s) \tag{21}$$

Substituting Equation (21) into (15), the transfer function from disturbance to state can be rewritten as:

$$\frac{1}{\varepsilon} = \left\| \begin{array}{c} W_1^{-1} K_{FINAL}(p) W_2^{-1} \left(I + G W_1^{-1} K_{FINAL}(p) W_2^{-1}\right)^{-1} M^{-1} \\ \left(I + G W_1^{-1} K_{FINAL}(p) W_2^{-1}\right)^{-1} M^{-1} \end{array} \right\|_\infty \tag{22}$$

PSO is a computational method that optimizes the problem as the organized movement style in a bird flock. The particles of PSO move around the search space until the stop

setting condition is met. Although the movement pattern of each particle is influenced by the local best position, it can update the new value if the other particle finds better position. Therefore, this leads to the movement of the swarm toward the best solution [21]. The proposed controller is evaluated by using the PSO algorithm, which is the fast and easy method to program without the complex mathematical analysis for solving the nonlinear robust H_∞ loop shaping problem. The proposed method sets the inverse Equation (22) to be the fitness function of PSO. Therefore, the cornerstones of controller design with PSO can be summarized as follows.

- Specify the controller parameter structure $K(p)$, p as the set of the controller parameters. The controller structure in this paper is specified as the simple structure PID in which Kp, Ki, Kd and τ_d are set as the family of the particle in PSO.

$$K(p) = Kp + \frac{Ki}{s} + \frac{Kds}{\tau_d s + 1} \tag{23}$$

  Set up the initial parameters of particle swarm optimization in the first iteration (number of particles, velocity, particle acceleration and moment of inertia, including the boundary of parameter in set p $[p_{\min}, p_{\max}]$).
- Start the swarm movement in the first iteration randomly and then evacuate the fitness value of each particle, while the inverse of the transfer function in Equation (22) is applied to being the fitness function of the PSO optimization.
- Update the inertia weight (J), position and velocity of each particle as:

$$J = J_{\max} - \left(\frac{J_{\max} - J_{\min}}{i_{\max}} \right) i \tag{24}$$

$$v_{i+1} = Q_{vi} + \alpha_1[\gamma_{1i}(P_b - p_i)] + \alpha_2 \tag{25}$$

  Update the position (p) and velocity (v) of each particle.

$$p_{i+1} = p_i + v_{i+1} \tag{26}$$

  where α_1, α_2 are the specified acceleration coefficients and γ_{1i} is the real numbers by the random search.
- Return to previous step, if the current iteration is less than the maximum iteration; otherwise, stop the swarm operation. The particle which achieves the maximum fitness value is the answer to this problem.

4. **Adaptive Notch Filter Using PSO.** The fixed structure robust controller (FSRC) can satisfy the uncertainty boundary of stability margin; however, it is still not effective enough for the perturbation plant that the frequencies shifted far away from the nominal resonance frequencies. The peak gain of the resonance shifted plant may cause the oscillation of output response and degrade the actuator performance. In this paper, the adaptive notch filter is presented to work with the robust fixed-structure PID controller as described in Section 3.3 in order to reduce the effect of the internal and external disturbances. These lead to an increase of the robustness and performance of the hard disk servo system.

In general, a shift of the resonance frequencies is caused by the environmental change of the hard disk drive. Thus, the fixed notch filters are not enough to attenuate the effect of various vibrations in hard disk drive with this condition. As seen in Figure 7, the frequencies of fixed notch filter cannot match the resonance of perturbation plant which causes the oscillation in the track seeking and following mode. Therefore, the adaptive notch filter which can track the frequency changing of the disturbed plant is utilized to combine in high performance controller.

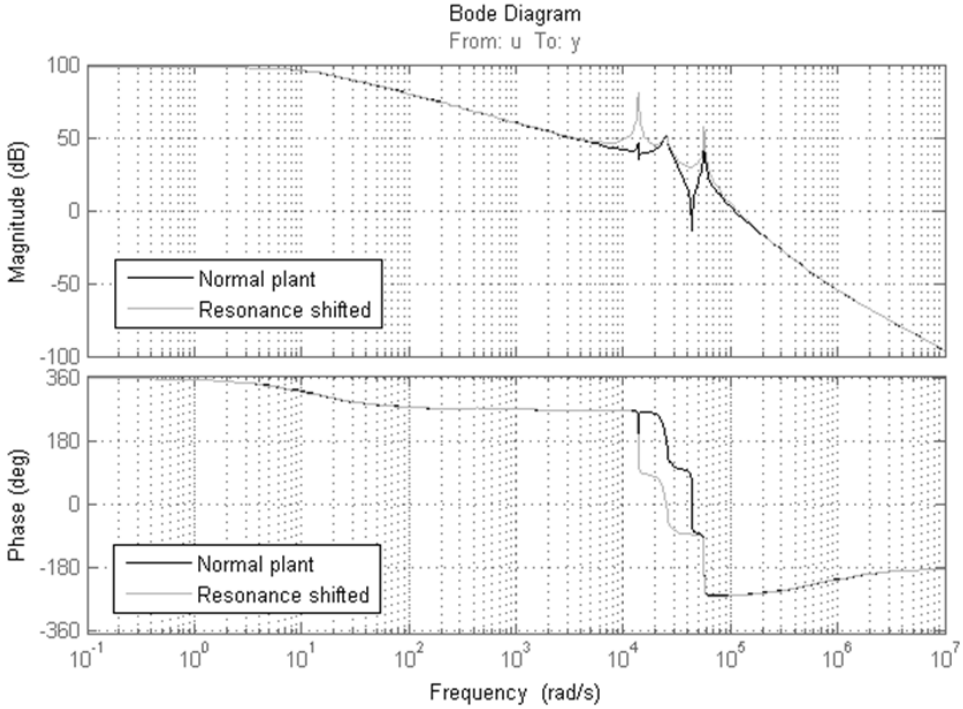

FIGURE 7. The frequency response of nominal plant and the plant with resonance shifted

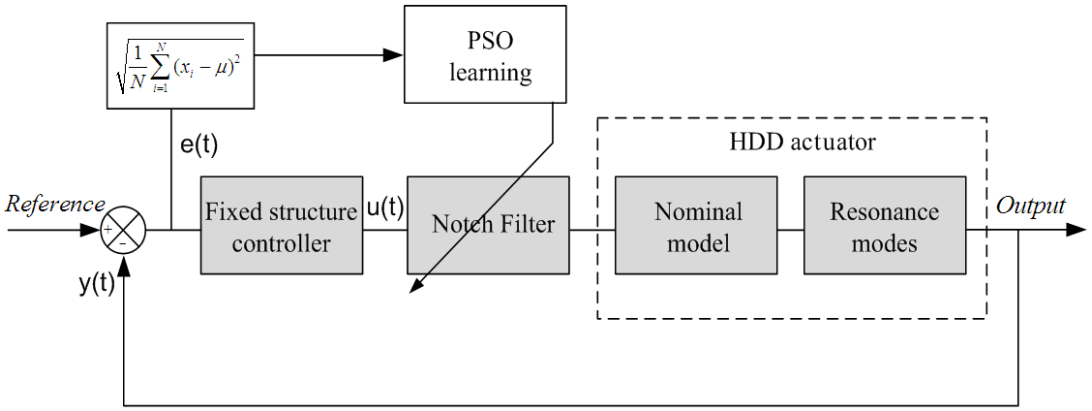

FIGURE 8. The adaptive notch filter diagram with the fixed structure controller

Figure 8 shows the proposed adaptive notch filter diagram along with robust fixed-structure controller. The figure demonstrates the adaptive notch filter that requires only to PES evaluate the parameters of notch filter into the adaptation block. The notch filter in this paper requires two frequency notch filters because there are two major resonances existing in the frequency response of VCM actuator.

$$notch(s) = \frac{s^2 + 2\xi_1\omega_1 s + \omega_1^2}{s^2 + 2\xi_{n1}\omega_1 s + \omega_1^2} \frac{s^2 + 2\xi_2\omega_2 s + \omega_2^2}{s^2 + 2\xi_{n2}\omega_2 s + \omega_2^2} \tag{27}$$

where ξ_1, ξ_{n1} and ξ_2, ξ_{n2} are the designed damping ratio values, while ω_1 and ω_2 are the frequency values of two resonance modes during 10^3 to 10^5 rad/s.

This paper aims to design an adaptive notch filter by using the particle swarm optimization to examine a set of notch filter parameters $\{\xi_1, \xi_{n1}, \xi_2, \xi_{n2}, \omega_1, \omega_2\}$ of Equation

(27) in order to compensate the impact of the major shifted resonances.

$$\left[\begin{array}{c} Adaptation \\ Fitness \end{array}\right] = \sqrt{\frac{1}{N}\sum_{i=1}^{N}(x_i-\mu)^2}, \quad \text{where } \mu = \frac{1}{N}\sum_{i=1}^{N} x_i \tag{28}$$

where N is the number of sampling data and x is the value of PES output error.

The SD and 3σ (3 standard deviation) of PES are widely used to identify the reference tracking performance of the actuator; therefore, the SD of the position output error of the actuator in Equation (28) is specified as the fitness function for the PSO optimization. Generally, the normal PSO algorithm is used to find the global best solution. In this paper, the $3\sigma_{PES}$, lower than the TMR budget of industry specification, is defined as the stopping condition in the adaptation process. If the adaptive system can detect the resonances shifted with indirect SD measurement value over the setting target, the proposed adaptive technique is returned to the adaptive loop process as the PSO adaptation flowchart in Figure 9.

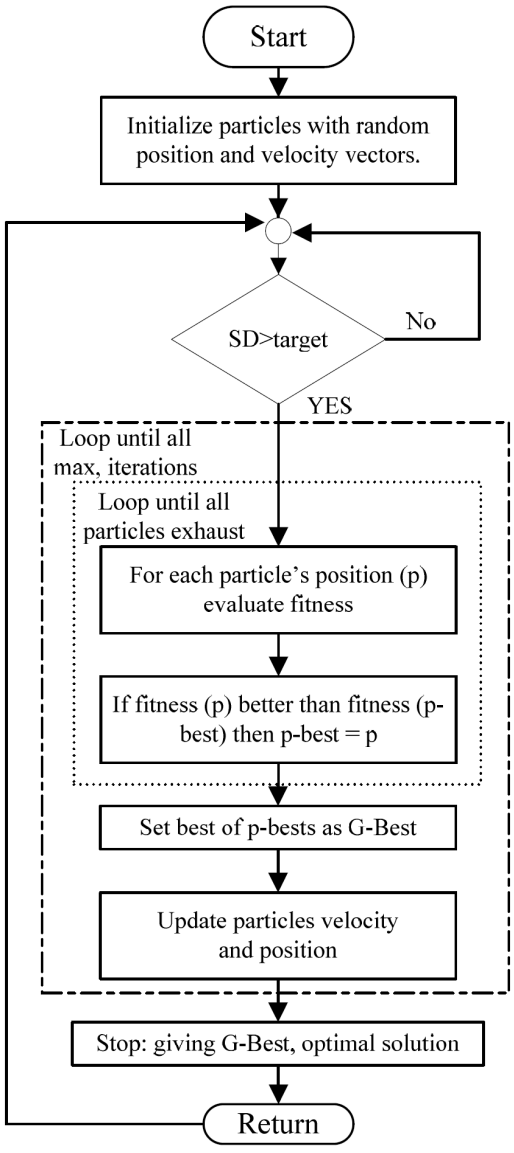

FIGURE 9. Adaptive notch filter based particle swarm optimization flowchart

As seen in the step to design the adaptive notch filter, the complex mathematical problem solving is not required for this proposed technique. Only the $3\sigma_{PES}$ objective function is the majority in this method in order to decide the next step direction of adaptation process. Therefore, this technique requires the computational time less than the other techniques such as fast Fourier transform (FFT) which uses high computational time calculation.

5. **Controller Design and Adaptive Notch Filter Results.** In this paper, H_∞ controller was designed based on the concept of weight selection under loop shaping procedure. The pre/post weight functions W_1 and W_2 are selected as:

$$\begin{bmatrix} W_1 \\ W_2 \end{bmatrix} = \begin{bmatrix} \dfrac{0.01545s + 19781}{s + 65000} \\ \dfrac{s + 10114.83}{s + 79591.83} \end{bmatrix} \tag{29}$$

Based on the optimization problem, PSO is adapted to search the controller parameters in sets of $K(p)$. $K(p)$'s parameter ranges are selected as the low gain controller (less than 1) in order to suppress the high gain behavior of the HDD plant; therefore, the upper and lower bounds of set p of the controller K can be chosen as: $K_p \in [0, 0.1]$, $K_i \in [0, 0.1]$, $K_d \in [0, 0.1]$, $\tau_d \in [1, 100]$, population size = 17, min-max velocities are 1 and 3, respectively, acceleration value = 2.1, min and max inertia are 0.1 and 0.5, respectively, iteration limit as 100. Finally, the proposed optimal solution with PID structure, which achieves a stability margin = 0.5865, can be written as:

$$K(p) = 0.002224 + \frac{0.042476}{s} - \frac{0.00196s}{s + 7944} \tag{30}$$

The controller designed by the conventional technique is the fourteen controller order to achieve the robustness of entire system. The maximum and H_∞ controller stability margin values are $\varepsilon_{\max} = 0.6417$ and $\varepsilon_{H_\infty} = 0.632$, respectively. The H_∞ loop shaping controller is illustrated as:

$$\begin{aligned} & K_{\infty VCM}(s) \\ &= \left\{ \frac{\begin{array}{c} 0.9336s^{14} + 1.849 \times 10^5 s^{13} + 2.009 \times 10^{10} s^{12} + 1.71 \times 10^{15} s^{11} \\ + 1.053 \times 10^{20} s^{10} + 5.135 \times 10^{24} s^9 + 2.037 \times 10^{29} s^8 + 5.703 \times 10^{33} s^7 \\ + 1.485 \times 10^{38} s^6 + 2.371 \times 10^{42} s^5 + 4.144 \times 10^{46} s^4 + 2.8 \times 10^{50} s^3 \\ + 3.766 \times 10^{54} s^2 + 2.128 \times 10^{56} s + 7.237 \times 10^{59} \end{array}}{\begin{array}{c} s^{14} + 1.996 \times 10^5 s^{13} + 2.178 \times 10^{10} s^{12} + 1.83 \times 10^{15} s^{11} \\ + 1.14 \times 10^{20} s^{10} + 5.458 \times 10^{24} s^9 + 2.195 \times 10^{29} s^8 + 6.024 \times 10^{33} s^7 \\ + 1.566 \times 10^{38} s^6 + 2.487 \times 10^{42} s^5 + 4.208 \times 10^{46} s^4 + 2.926 \times 10^{50} s^3 \\ + 3.685 \times 10^{54} s^2 + 2.138 \times 10^{56} s + 7.045 \times 10^{59} \end{array}} \right\} \end{aligned} \tag{31}$$

The open loop bode is utilized to evaluate the robust performance in terms of frequency response. The proposed design, the H_∞ loop shaping and the shaped plant bode results are illustrated in Figure 10(a), while the tracking performance results of each controller are compared in Figure 10(b). Moreover, Figure 10(c) shows the robust disturbance attenuation and performance tracking in terms of singular value of sensitivity function (S) and complementary sensitivity function (T), additionally, the results show peak gain of S = 1.73 dB and T = 0.05 dB while the crossover frequency exists around 10^4 rad/s. The outcomes show the similarity between the effectiveness of the proposed response and the H_∞ controller with high order. Besides, the stabilities of these two systems are almost the same. The summarized details of these step responses are also described in Table 2.

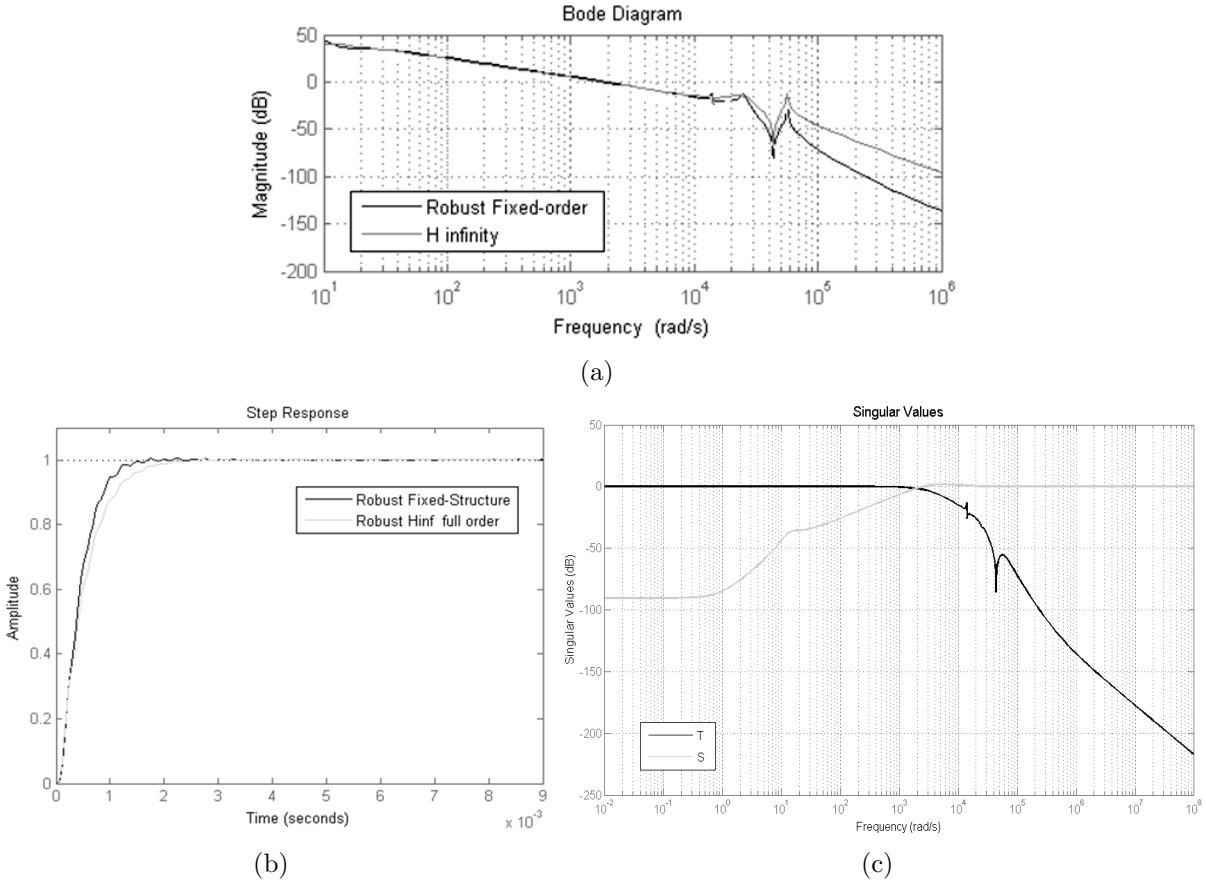

FIGURE 10. The results of (a) bode open loop frequency response of the controllers; (b) step responses of the controllers; (c) singular value of S and T of the proposed controller

TABLE 2. The performance and robustness specifications of the proposed designed controller

Controller	**Order**	**Settling time**	**Overshoot**	**Stability margin**
Full order H_∞ controller	14	2.1 ms	0.08%	0.632
Fixed structure PID controller	2	1.2 ms	0.05%	0.5865

In the part of the adaptive notch filter, the parameters of notch appearing in Equation (27) corresponding to the base and center of the notch frequency are updated for matching the frequency shifted from the VCM plant perturbation. Figure 11 shows the step responses of the nominal scenario with FFNF (black line) compared to the disturbed plant, which produces a large overshoot but still stable (light gray line).

The frequency of the disturbed plant is shifted by 60% of the major mechanical resonance frequencies of the VCM, and the step responses corresponding to open loop singular value are shown in Figures 12 and 13. These figures illustrate the adaptation processes of PSO in each iteration until the frequencies of adaptive notch filter are matched around the center of mechanical frequency shifted. In addition, the adaptation of the proposed algorithm will be stopped when the fitness of PSO is lower than the threshold value (as seen in Figures 12 and 13). Figure 14 shows the Gbest values versus iterations of the proposed adaptive notch filter.

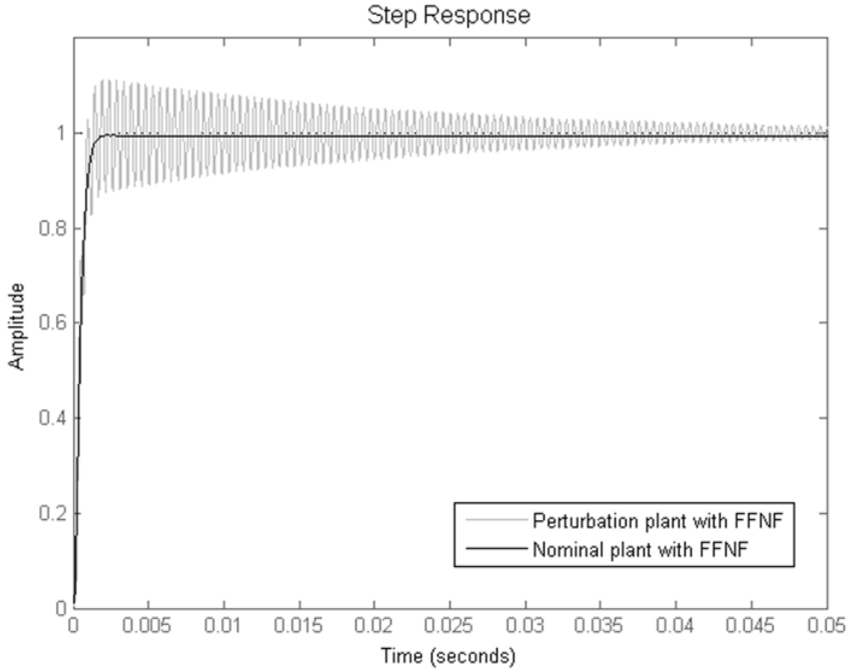

FIGURE 11. Step response of the nominal and perturbation plants with fixed frequency notch filter (FFNF)

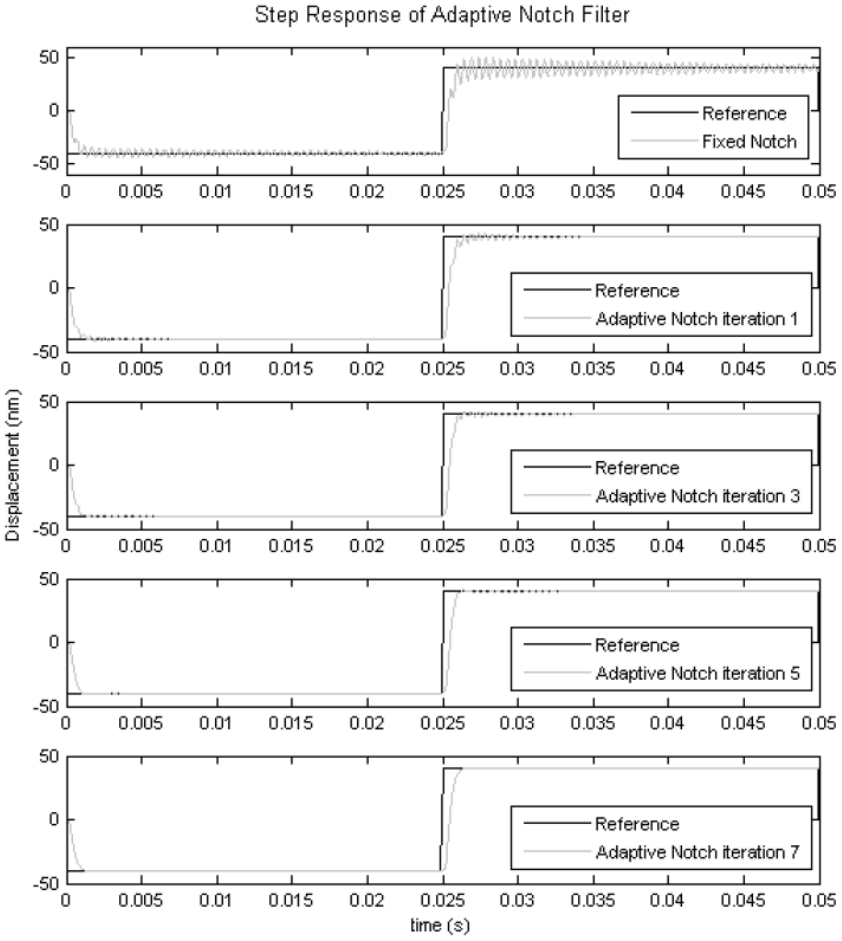

FIGURE 12. The step responses of the proposed algorithm during the adaptation process

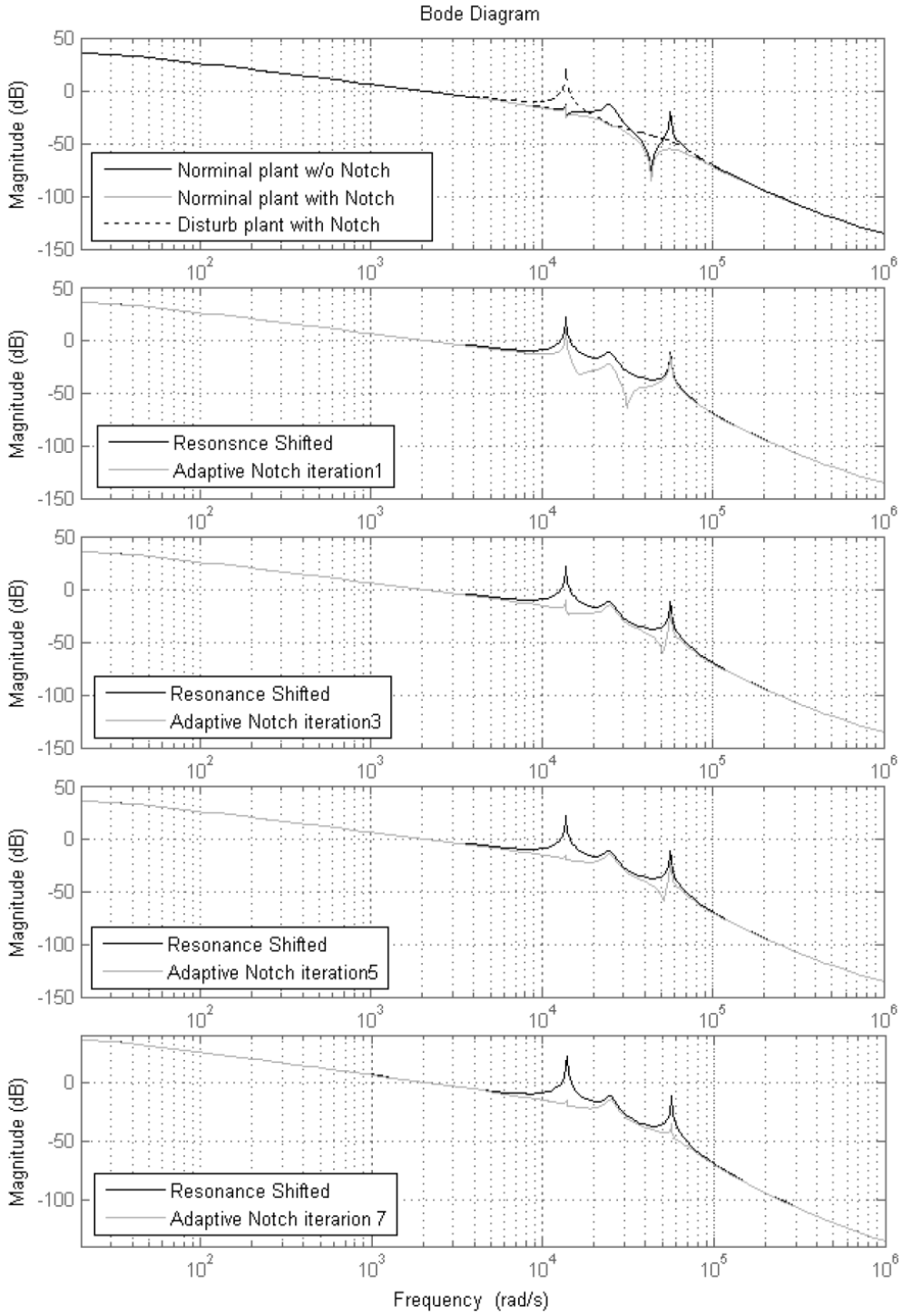

FIGURE 13. The frequency responses of the proposed algorithm during the adaptation

In order to evaluate the performance of the proposed design, six scenarios resonance shifted between 10%-65% are tested and compared with the conventional FFNF as seen in Figure 15. The importance results are concluded in Table 3 of the appendix section. The results also substantiate the effectiveness of the fixed structure controller and adaptive notch filter, which does not only increase the tracking performance, but also reduce the oscillation of resonance shifted effect as well.

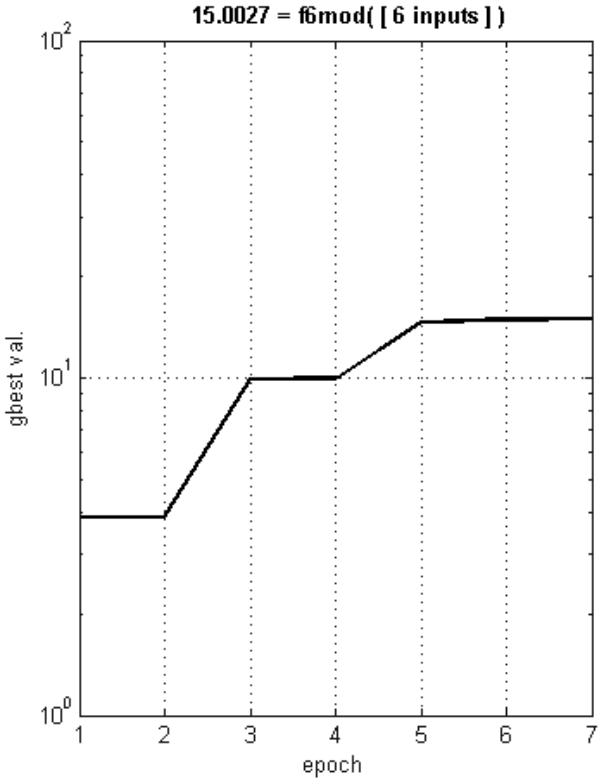

FIGURE 14. Gbest values versus iterations in the particle swarm optimization of adaptive notch filter

6. **Conclusion.** The fixed-structure PID based H_∞ robust loop shaping and the adaptive notch filter for voice coil motor (VCM) of hard disk drive system are proposed in this paper. The robustness and performance of the H_∞ robust loop shaping procedure are defined by single index, stability margin (ε) which is utilized as the objective function of the proposed particle swarm optimization algorithm to solve the inherently non-convex nonlinear problem based proposed PID structure. Although the stability margin of the conventional H_∞ robust loop shaping is more than the proposed method, the order of the proposed controller is less than that of the conventional H_∞ full order. The simple structure as the PID leads to easier implementation and reduces the computational time of the calculation process. The results of the proposed controller with specified open loop shape illustrate the potential of tracking performance and also guarantee the robust stability of the system; nevertheless, the proposed fixed structure controller is not robust enough for the perturbation plant which the centers of resonances are shifted far away from the nominal, which causes an increase of vibration in positioning system. Therefore, the combination of the adaptive notch filter and the fixed-structure H_∞ robust loop shaping approaches is proposed to suppress the resonance shifted in VCM actuator. The parameters of the base and center of the notch filters are considered to degrade the effect of each resonance shifted. Simulation results with six scenario tests clearly demonstrate the effectiveness of the proposed technique over the conventional fixed-frequency notch filter.

Acknowledgments. This research work is supported by Faculty of Engineering, King Mongkut's Institute of Technology Ladkrabang and the Thailand Research Fund under the research grant no. PHD57I0052.

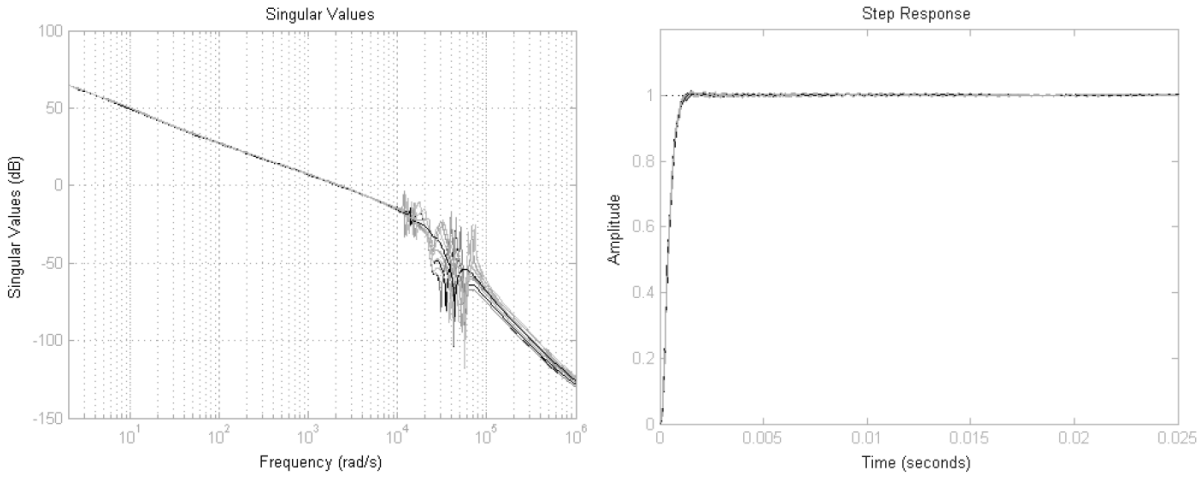
Singular Values
Singular Values (dB)
Frequency (rad/s)
Step Response
Amplitude
Time (seconds)

(a)

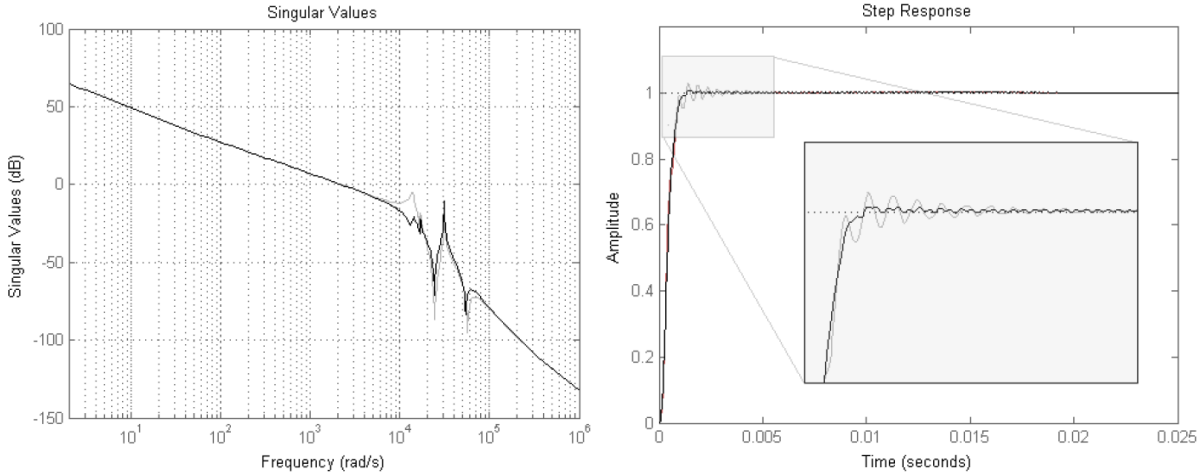
Singular Values
Singular Values (dB)
Frequency (rad/s)
Step Response
Amplitude
Time (seconds)

(b)

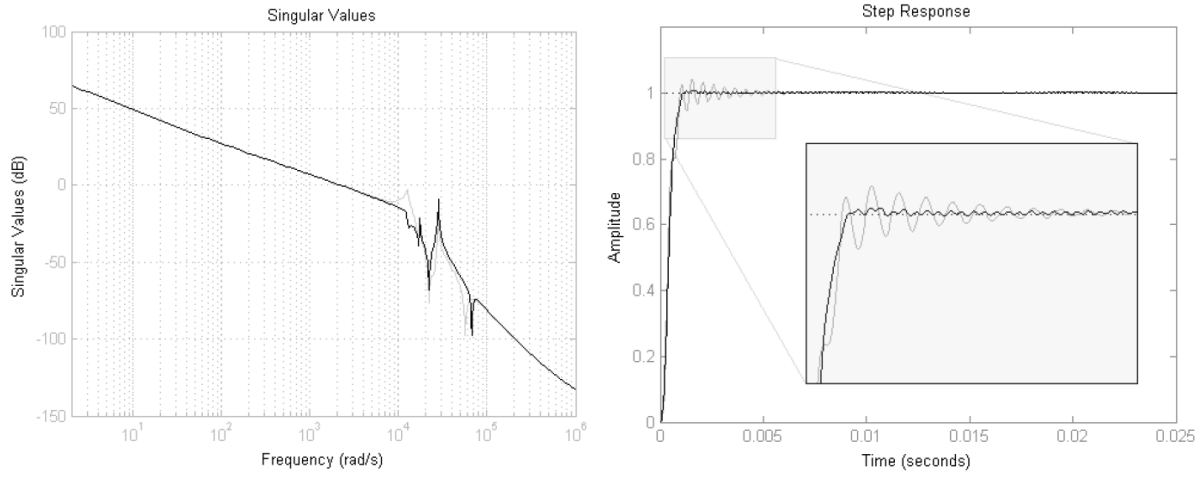
Singular Values
Singular Values (dB)
Frequency (rad/s)
Step Response
Amplitude
Time (seconds)

(c)

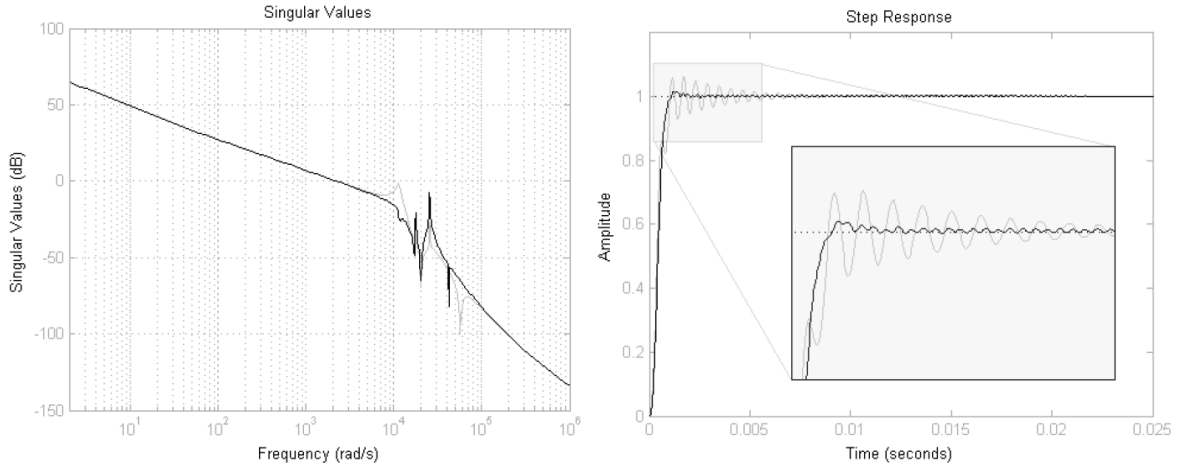

(d)

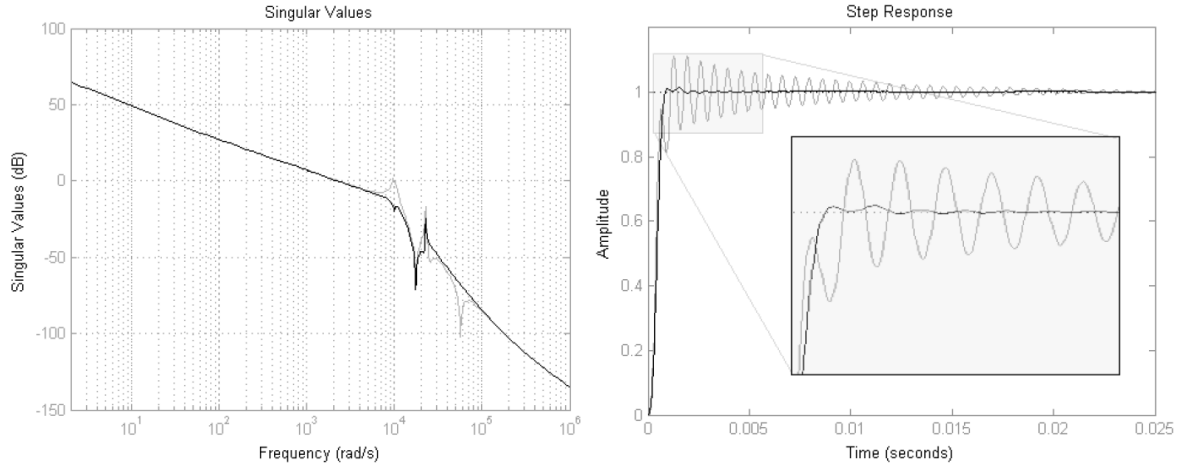

(e)

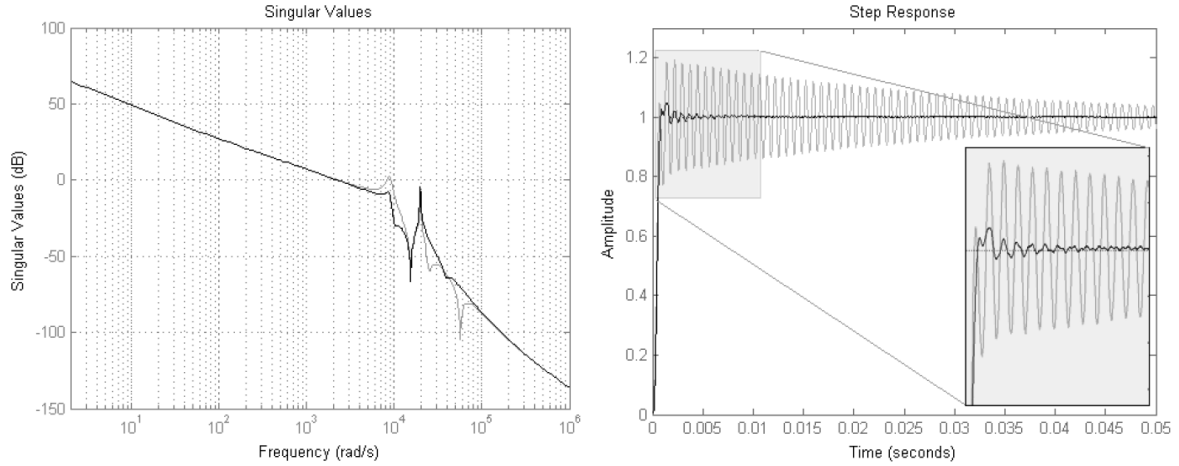

(f)

FIGURE 15. The comparison in terms of step response and singular value of six scenarios test results (light gray line denotes fixed-frequency-notch filter: FFNF and black line denotes proposed adaptive notch filter: ANF): (a) Scenario 1: 10%-40% resonances shifted with 64 random cases, (b) Scenario 2: 45% resonances shifted, (c) Scenario 3: 50% resonances shifted, (d) Scenario 4: 55% resonances shifted, (e) Scenario 5: 60% resonances shifted, (f) Scenario 6: 65% resonances shifted

TABLE 3. Six scenarios test results of fixed frequency notch filter (FFNF) and proposed adaptive notch filter

Scenarios of resonance shifted	Adaptation process	Rise time (ms)		Settling time (ms)		Overshoot (%)		Sum square error (pu.)	
		FFNF	ANF	FFNF	ANF	FFNF	ANF	FFNF	ANF
10%-40% shifted	No	0.89	–	1.2	–	0.15	–	0.84	–
45% shifted	Active	0.85	0.92	2.8	1.22	3.06	0.62	0.99	0.85
50% shifted	Active	0.86	0.87	4.2	0.93	4.37	0.60	1.06	0.86
55% shifted	Active	0.92	0.91	6.4	1.23	6.46	1.83	1.17	0.89
60% shifted	Active	1.01	0.93	20.5	2.16	11.34	1.67	1.49	0.91
65% shifted	Active	0.53	0.54	81.2	5.42	18.76	4.31	3.74	1.15

REFERENCES

[1] L. Zhang, K. Yao and Y. F Chen, Dual-stage nano-positioning scheme for 10 Tbit/in2 hard disk drives with a shear-mode piezoelectric single-crystal microactuator, *IEEE Trans. Magnetics*, vol.51, no.4, pp.1942-1948, 2015.

[2] B. M. Chen, T. H. Lee, K. Peng and V. Venkataramanan, *Hard Disk Drive Servo Systems*, 2nd Edition, Springer, 2005.

[3] A. Al-Mamun, G. Guo and C. Bi, *Hard Disk Drive Mechatronics and Control*, CRC Press, 2006.

[4] G. F. Franklin, J. D. Powell and M. L. Workman, *Digital Control of Dynamic System*, 3rd Edition, Addison-Wesley, 1997.

[5] S. Skogestad and I. Postlethwaite, *Multivariable Feedback Control Analysis and Design*, 2nd Edition, John Wiley & Sons, 1996.

[6] K. Zhou and J. C. Doyle, *Essential of Robust Control*, Prentice-Hall, 1998.

[7] D. C. McFarlane and K. Glover, A loop shaping design procedure using H_∞ synthesis, *IEEE Trans. Automatic Control*, vol.37, no.6, pp.759-769, 1992.

[8] S. S. Aphale, S. O. R. Moheimani and A. Ferreira, A robust loop-shaping approach to fast and accurate nano-positioning, *Sensors and Actuators A: Physical*, pp.88-96, 2013.

[9] S. Kaitwanidvilai and M. Parnichkun, Genetic algorithm based on fixed-structure robust H_∞ loop shaping control for pneumatic servo system, *Journal of Robotics and Mechatronics*, vol.16, no.4, pp.362-373, 2004.

[10] S. Khan, S. Yang and O. U. Rehman, A global particle swarm optimization algorithm applied to electromagnetic design problem, *International Journal of Applied Electromagnetics and Mechanics*, pp.1-17, 2016.

[11] S.-H. Lee and C. C. Chung, Optimal design and testing of a digital dual-stage actuator servo system, *IET Control Theory and Applications*, vol.4, pp.2029-2040, 2010.

[12] H. Li, C. Du and Y. Wang, Optimal reset control for a dual-stage actuator system in HDDs, *IEEE Trans. Mechatronics*, vol.16, pp.480-488, 2011.

[13] J. Nie, E. Sheh and R. Horowitz, Optimal H_∞ control design and implementation of hard disk drives with irregular sampling rates, *IEEE Trans. Control Systems Technology*, vol.20, no.2, pp.402-407, 2012.

[14] S. Kaitwanidvilai and A. Nath, Design and implementation of a high performance hard disk drive controller using GA based 2DOF robust controller, *International Journal of Innovative Computing, Information and Control*, vol.8, no.2, pp.1025-1036, 2012.

[15] Y. Shinohara, K. Seki and M. Iwasaki, Robust vibration suppression control for resonant frequency variations in dual-stage actuator-driven load devices, *IEEE International Conference on Mechatronics (ICM)*, pp.632-637, 2015.

[16] K. J. Astrom and B. Wittenmarl, *Adaptive Control Systems*, Addison Wesley, 1995.

[17] J. C. Tudon-Martinez and R. Morales-Menendez, An adaptive disturbance rejection method with stability enhancement using adjustable dead-zone for hard disk drives, *IEEE Trans. Magnetics*, pp.1-10, 2016.

[18] C. I. Kang and C. H. Kim, An adaptive notch filter for suppressing mechanical resonance in high track density disk drives, *Microsystem Technology*, vol.11, pp.638-652, 2005.

[19] K. P. Tee, S. S. Ge and E. H. Tay, Adaptive resonance compensation for hard disk drive servo systems, *Proc. of IEEE Conference on Decision and Control*, pp.3567-3572, 2007.
[20] P. P. Sant, *Modelling and Control of Hard Disk Drive in Mobile Applications*, Master Thesis, Department of Electrical and Computer Engineering, National University of Singapore, 2009.
[21] J. Kennedy and R. Eberhart, Particle swarm optimization, *Proc. of IEEE International Conference on Neural Networks*, Perth, Australia, pp.1942-1948, 1995.